

Journal Pre-proofs

Engineering micro- and nanosized pharmaceutical salt crystals using high-pressure homogenization

Md Sadeque Hossein Mithu, Saumil Bhatt, Vivek Garg, Vivek Trivedi, Dennis Douroumis

PII: S0378-5173(26)00093-1
DOI: <https://doi.org/10.1016/j.ijpharm.2026.126645>
Reference: IJP 126645

To appear in: *International Journal of Pharmaceutics*

Received Date: 4 December 2025
Revised Date: 29 January 2026
Accepted Date: 30 January 2026

Please cite this article as: M.S. Hossein Mithu, S. Bhatt, V. Garg, V. Trivedi, D. Douroumis, Engineering micro- and nanosized pharmaceutical salt crystals using high-pressure homogenization, *International Journal of Pharmaceutics* (2026), doi: <https://doi.org/10.1016/j.ijpharm.2026.126645>

This is a PDF of an article that has undergone enhancements after acceptance, such as the addition of a cover page and metadata, and formatting for readability. This version will undergo additional copyediting, typesetting and review before it is published in its final form. As such, this version is no longer the Accepted Manuscript, but it is not yet the definitive Version of Record; we are providing this early version to give early visibility of the article. Please note that Elsevier's sharing policy for the Published Journal Article applies to this version, see: <https://www.elsevier.com/about/policies-and-standards/sharing#4-published-journal-article>. Please also note that, during the production process, errors may be discovered which could affect the content, and all legal disclaimers that apply to the journal pertain.

© 2026 Published by Elsevier B.V.



1
2
3
4
5
6
7
8
9
10
11
12
13
14
15
16
17
18
19
20
21
22
23
24
25
26
27
28

Engineering Micro- and Nanosized Pharmaceutical Salt Crystals Using High-Pressure Homogenization

**Md Sadeque Hossein Mithu¹, Saumil Bhatt¹, Vivek Garg⁴, Vivek Trivedi³,
Dennis Douroumis^{1,2}**

¹Cubic Pharmaceuticals Ltd., Unit 3, Neptune Close, Medway City Estate, Rochester, Kent, ME2 4LU, UK

²School of Life and Health Sciences, Department of Health Sciences, Pharmacy, University of Nicosia, No. 17, 29th Street, Elliniko 167 77, Athens, Greece

³Medway School of Pharmacy, University of Kent, Medway Campus, Central Avenue, Chatham Maritime, Chatham, Kent ME4 4TB, United Kingdom

⁴Wolfson Centre for Bulk Solids Handling Technology, Faculty of Engineering & Science, University of Greenwich, Central Avenue, Chatham ME4 4TB, UK

Abstract

1 This study presents an innovative application of high-pressure homogenization (HPH) for the
2 synthesis of micro- and nanocrystalline pharmaceutical salts, offering a scalable and
3 environmentally sustainable alternative to conventional crystallization techniques. Using
4 ketoconazole (KTZ) and oxalic acid (OA) as a model system, salt formation was successfully
5 achieved through HPH processing in the presence of various stabilizers (Pharmacoat® 606,
6 Pluronic® F127, Soluplus®, and TPGS) at different concentrations and process temperatures.
7 Structural analysis by XRPD and FT-IR confirmed the formation of a new multicomponent
8 salt through proton transfer and hydrogen bonding, while SEM imaging revealed controlled
9 crystal morphology and significant particle size reduction to the submicron range. The process
10 demonstrated remarkable reproducibility and flexibility, allowing morphological tuning
11 through simple adjustments in stabilizer concentration and temperature. Dissolution studies
12 performed at pH 4.4 showed up to an 80% drug release within 15 minutes for HPH-processed
13 KTZ:OA salts, a substantial improvement over bulk KTZ. The findings establish HPH as a
14 versatile, solvent-free, and continuous manufacturing platform for the production of high-
15 purity pharmaceutical salts with superior dissolution performance, highlighting its potential to
16 transform solid-state drug formulation and process intensification strategies in pharmaceutical
17 development.

18 **Keywords:** Nanoparticles, microparticles, High Pressure Homogenization, Salts, Surfactants

19

20

21

22

23

24

25

26

1. Introduction

27 Nanosizing drug particles is a widely recognized strategy to improve the dissolution rate and
28 bioavailability of BCS class II drugs by increasing their surface area and saturation solubility
29 [1]. According to the Noyes–Whitney equation, enhanced solubility accelerates dissolution,
30 while higher drug concentration in the gastrointestinal lumen increases the concentration
31 gradient, promoting diffusion and absorption [2]. Nanosized formulations also require lower
32 excipient levels, achieving higher local drug concentrations while reducing potential excipient-
33 related toxicity [3]. Despite these advantages, only a limited number of nanocrystal-based
34 pharmaceutical products have reached the market, although further product launches are
35 anticipated [4]. In the United States, nanocrystal technology is featured in 85 active patents
36 with an additional 48 pending [5].

37 Another approach to increase drug solubility and hence dissolution rates especially for the
38 ionisable compounds. involves the formation of multicomponent products such as cocrystals
39 and salt [6,7]. There is a number of processing technologies that have been successfully
40 employed for the formation of multicomponent crystals, including solvent evaporation, slurry

1 crystallization, mechanochemical processing, antisolvent preparation, extrusion, and
2 supercritical fluid processing [8-12].

3 High-pressure homogenization (HPH) has emerged as an effective method to produce
4 nanosized drug particles, adapted from food and biotechnology applications [5-7, 13-17]. In
5 this process, a fluid product is forced through a narrow nozzle under high pressure, reducing
6 particle size and increasing surface area and free energy. However, particles below ~30 µm are
7 prone to aggregation due to van der Waals and electrostatic forces, which can decrease effective
8 surface area and negatively impact dissolution and bioavailability [18]. Polymers are
9 commonly employed as stabilizers during and after HPH to prevent agglomeration, while
10 simultaneously enhancing solubility, wettability, and bioavailability. Stabilizer selection is
11 typically empirical, with generally recognized as safe (GRAS) excipients widely used [4].

12 In this study, ketoconazole (KTZ) and oxalic acid (OA) were selected as a model API and salt
13 former to produce nanosized salt crystals via HPH. Four polymers—Pharmacoat® 606
14 (HPMC), Pluronic® F127, Soluplus®, and TPGS—were evaluated as stabilizers. HPMC has
15 been shown to produce nanocrystals as small as 70–120 nm for various APIs, with its
16 hydrophobic segments facilitating surface adsorption and particle stabilization [19,20].
17 Pluronic® F127, an amphiphilic block copolymer of polypropylene oxide and polyethylene
18 oxide, has demonstrated superior stabilization compared to traditional homopolymers and has
19 been used effectively in indomethacin and itraconazole nanosuspensions [21,22]. TPGS has
20 broad pharmaceutical applicability and has been successfully used to produce memantine-
21 pamoic acid nanocrystals via HPH [20,23]. Soluplus®, a graft copolymer composed of
22 polyethylene glycol, polyvinyl acetate, and polyvinyl caprolactam, has been employed in
23 celecoxib nanoparticle formation using anti-solvent precipitation combined with HPH [24].
24 The KTZ:OA salt (stoichiometric ratio 1:1.1) has previously been prepared via solvent
25 evaporation and slurry crystallization, providing a suitable model system for nanosizing studies
26 [25,26].

27 Overall, HPH combined with appropriate polymer stabilizers offers a versatile and scalable
28 approach to produce stable nanosized pharmaceutical salts, enhancing dissolution, solubility,
29 and ultimately bioavailability.

30

31 **2. Materials and methods**

32 **2.1 Materials**

33 Ketoconazole (KTZ), oxalic acid (OA), Pluronic® F-127, and **D-α-tocopheryl polyethylene**
34 **glycol 1000 succinate** (TPGS) were purchased by Sigma-Aldric, UK. Soluplus® (Polyvinyl
35 caprolactame- polyvinyl acetate-polyethylene glycol graft) was kindly donated by BASF
36 (Germany). Reagents of HPLC grade such as methanol and acetonitrile were purchased from
37 Fisher Chemicals (Loughborough, UK). The solids and solvents were used as received without
38 further purification.

39

40 **2.2 High-pressure homogenisation**

41 High pressure homogenization was employed for the processing of the drug and salt former
42 solutions for the synthesis of the salts. Specifically, **physical mixtures (1 g) of KTZ and OA**

1 (stoichiometric ratio 1:1.1) were dissolved in a solvent mixture (2% w/v) of acetone and
 2 methanol (1:1) and then homogenised in 50 mL of the aqueous phase (with or without the
 3 stabilizers). The role of various polymers as stabilisers was investigated; for this purpose,
 4 0.25% and 0.50% (w/v) of polymers were added to the aqueous phase and stirred for 30 min
 5 until were fully dissolved (Table 1). After the addition of polymer, the resulting clear solution
 6 was rapidly transferred and homogenised in a MicroDebee laboratory homogeniser (South
 7 Easton, MA, USA) at 15000 psi for a predetermined time at room temperature. The
 8 homogenization process was repeated for selected formulations this time by applying
 9 temperatures of 40 °C for the same period (Table 2). At the end of the homogenisation process,
 10 the samples were subjected to vacuum filtration using a borosilate Buchner kit (Millipore
 11 XX1004700) with PTFE (polytetrafluoroethylene) filters (0.1 µm) to remove the
 12 aqueous/organic solutions. The process was applied for another 10 min to dry the cocrystals.
 13 The filtrate was dried overnight at 50 °C and stored for further analysis.

14 **Table 1:** Different formulations of KTZ and oxalic acid with various polymers and
 15 surfactants.

Exp. No	Stabilizers	Amount (w/v%)	Temp. (°C)	Drug/former: stabilizer ratio
1	Pharmacoat 606	0.25	25.0	4:1
2	Pharmacoat 606	0.50	25.0	3:1
3	Pluronic F127	0.25	25.0	4:1
4	Pluronic F127	0.50	25.0	3:1
5	Soluplus	0.25	25.0	4:1
6	Soluplus	0.50	25.0	3:1
7	TPGS	0.25	25.0	4:1
8	TPGS	0.50	25.0	3:1

16

17 **Table 2:** Different formulations of KTZ and OA with various polymers and surfactants.

1 at 40 °C

Exp. No	Stabilizers	Amount (w/v%)	Temperature (°C)	Drug/former: stabilizer ratio	Hansen solubility parameter (δ , MPa ^{1/2})
9	Pharmacoat 606	0.5	40	3:1	27.8
10	Pluronic F127	0.5	40	3:1	21.0
11	Soluplus	0.5	40	3:1	20.7
12	TPGS	0.5	40	3:1	23.8

2 δ_{KTZ} : 25.4 MPa^{1/2}

3 2.3. Differential scanning calorimetry (DSC)

4 Bulk compounds, physical mixture (PM) of API and coformer and collected solid products
5 from three different processing by HPH were analysed using a DSC (Mettler Toledo 823e,
6 Greifensee, Switzerland). All the samples were accurately weighed (2 to 4 mg) and placed into
7 aluminium pans and transferred to the sample holder. Samples were then heated over the
8 required temperature range (depending on their melting point), starting from 0°C or 25°C up
9 to 300°C at a scan rate of 10 °C/min under an atmosphere of nitrogen gas using a flow of 50
10 mL/min. STARe software was used to analyse the data obtained from the samples.

11

12 2.4. Powder X-ray diffraction (PXRD)

13 PXRD data of all the bulk samples, PM and final products prepared by HPH processing were
14 collected using a D8 Advanced X-ray diffractometer (Bruker, Germany). A Cu anode powered
15 at 40 kV and 40 mA, a primary 4° Soller slit and a secondary 2.5° Soller slit, and a 0.2 mm exit
16 slit was selected for all experiments. The samples were rotated at 15 RPM (rotation per minute)
17 with a step size set at 0.02 °2 θ and the counting time set at 0.2 sec per step. Few milligrams of
18 dried solids were placed on a sample holder and diffractograms were collected at a range of 2-
19 55 °2 θ scale. A primary Göbel mirror was used for the parallel beam and the removal of Cu
20 K β . EVA phase analysis (Bruker, Germany) software was used to analyse the data and
21 compare the peak positions.

22

1 2.5 Cambridge structural database (CSD) search

2 All searches were carried out in the Cambridge structural database (CSD, Cambridge
3 Crystallographic Data Centre). The search for ketoconazole cocrystals and salt was done by
4 typing ketoconazole in compound name option in the access structure site. There were only
5 two hits, which were not cocrystal/salt. Based on the published work of Martin et al. (2013)
6 yielded four CIF files: ketoconazole cocrystals with fumaric (YINWAV), succinic (YINWEZ),
7 and adipic (YINWID) acids, and ketoconazole oxalate salt (YINVUO). These were used in
8 PXRD analysis with TOPAS to assess cocrystal and salt formation.

9

10 2.6. FTIR spectroscopy analysis

11 ATR-FTIR spectroscopy was performed for both the API and conformer, as well as for the
12 solids obtained from the process using HPH, with a PerkinElmer Spectrum Two (UK) equipped
13 with a ZnSe crystal. The ATR crystal, pressure plate, and tip were thoroughly cleaned before
14 each background and sample scan to avoid cross-contamination. A small amount of sample
15 was placed directly onto the crystal, and contact was ensured by adjusting the applied force
16 using the metal tip. Spectra were collected over the range of 400–4000 cm^{-1} at a resolution of
17 4 cm^{-1} , with four scans averaged per spectrum.

18 2.7 Scanning electron microscopy (SEM)

19 The morphology of ketoconazole, oxalic acid, and the HPH processed products was examined
20 using a SEM (Hitachi SU8030, Japan), operated at an accelerating voltage of 1 kV in
21 backscattering mode. A small amount of each sample was mounted onto an aluminium stub
22 using conductive adhesive and coated with a thin layer of chromium for approximately 3
23 minutes to enhance surface conductivity. Micrographs were acquired at various magnifications
24 to evaluate and compare the morphological features of the samples.

25

26 2.8 In-vitro dissolution studies

27 Dissolution studies were conducted using a USP paddle apparatus method by employing a
28 Varian 705 DS dissolution paddle apparatus (Varian Inc., North Carolina, US). Acetate buffer,
29 pH 4.4 (glacial acetic acid and anhydrous sodium trihydrate) was used as dissolution media,
30 the temperature was maintained at 37.5 ± 1 °C and the rotation speed of the shaft was set to 100
31 RPM. 100 mg of bulk KTZ and the equivalent amount of jet dispensed powder was placed into
32 the apparatus containing 900 mL buffer. 5 mL of the sample was withdrawn from the apparatus
33 after 15 minutes and it was replaced by 5 mL of buffer immediately. This process was repeated
34 at different time intervals: 15, 30, 60, 90 and 120 minutes. The collected samples were then
35 filtered and analysed by Agilent Technology 1200 series HPLC (Agilent Technologies,
36 Cheshire, UK) using a Hichrom S50DS2 - 4889, (4.6 mm x 150 mm) column and a freshly
37 prepared mobile phase consisting of methanol: water: triethylamine (80:20:0.02% v/v). The
38 analysis was performed at a mobile phase flow rate of 1 mL/min on 20 μL sample at 240 nm.
39 Collected data was analysed and integrated using Chemstation®.

40

41 2.9 Statistical analysis

1 Statistical analysis was performed for in-vitro dissolution performances of the synthesized salts
2 using the Two-way ANOVA, and statistical significance was set at $p < 0.05$ using Fusion One
3 software (DoE Fusion One TM, California, United States).

5 3. Results and discussion

6 3.1. HPH for nanocrystal salt synthesis

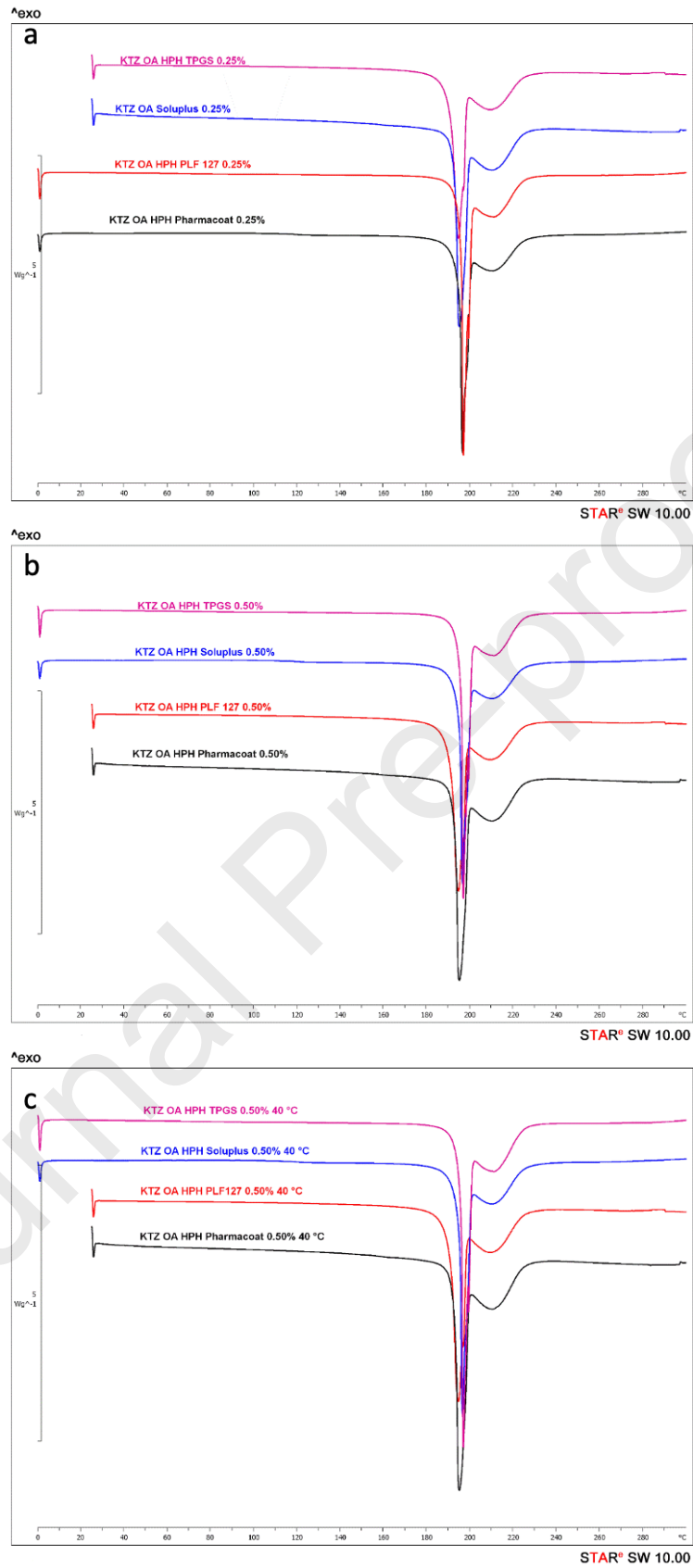
7 The formulation of poorly water-soluble active pharmaceutical ingredients (APIs) remains a
8 major challenge in modern drug development. Among various nanonization technologies,
9 nanocrystal production has emerged as an effective strategy to enhance dissolution rate,
10 saturation solubility, and oral bioavailability. High-Pressure Homogenization operates via
11 intense shear and cavitation forces under pressures up to 2000 bar, reducing coarse drug
12 suspensions to nanoscale dimensions. It is a solvent-free, scalable, and industry-preferred top-
13 down process that produces highly stable nanosuspensions with narrow particle size
14 distribution (typically 100–500 nm). Its reproducibility and compatibility with aqueous
15 stabilizers make it particularly suited for continuous manufacturing and regulatory compliance.

16 There are also other bottom-up precipitation approaches enable fine control over nucleation
17 and crystal growth, producing particles as small as 50–400 nm. However, solvent–antisolvent
18 systems complicate scale-up and solvent removal. Sonocrystallization for example combines
19 acoustic cavitation and supersaturation control, providing a versatile laboratory-scale method
20 for screening polymorphs and co-crystals, though limited by batch processing and energy
21 efficiency.

22 Among those technologies, HPH is a preferred approach due to its robust scalability,
23 environmental friendliness, and ability to integrate salt formation and particle size reduction
24 within a single process step. It has demonstrated success in generating nanocrystals of drugs
25 such as ketoconazole, fenofibrate, and itraconazole, leading to significantly improved
26 dissolution and bioavailability [27-29]. Overall, while all four methods offer distinct benefits,
27 HPH remains the most versatile and industrially adaptable nanocrystal production platform for
28 poorly soluble pharmaceuticals. Hence we introduce for first time the use of HPH for the
29 synthesis of salt nanocrystals by using KTZ:OA as model drug-former pair. The key processing
30 parameters were the applied pressure and temperature of the homogenizer that were considered
31 [30] for the salt synthesis and particle engineering. In addition, the aqueous/organic phase ratio
32 was another critical material attribute which was kept at 25:1 based on previous work [31].

33 3.2 Solid state analysis

34 DSC analysis was performed to investigate the thermal events occurred in the bulk solid and
35 freshly made cocrystals made by HPH process. Fig. 1a, illustrates the obtained thermograms



1

2 **Fig.1:** DSC thermograms of KTZ-OA homogenised at a) 0.25% (w/v) concentrations of
3 Pharmacoat®, Pluronic® 127, Soluplus® and TPGS at 25°C, a) 0.50% (w/v) concentrations of

1 Pharmacoat®, Pluronic® 127, Soluplus® and TPGS at 25°C and c) 0.50% (w/v)
2 concentrations of Pharmacoat®, Pluronic® 127, Soluplus® and TPGS at 40°C

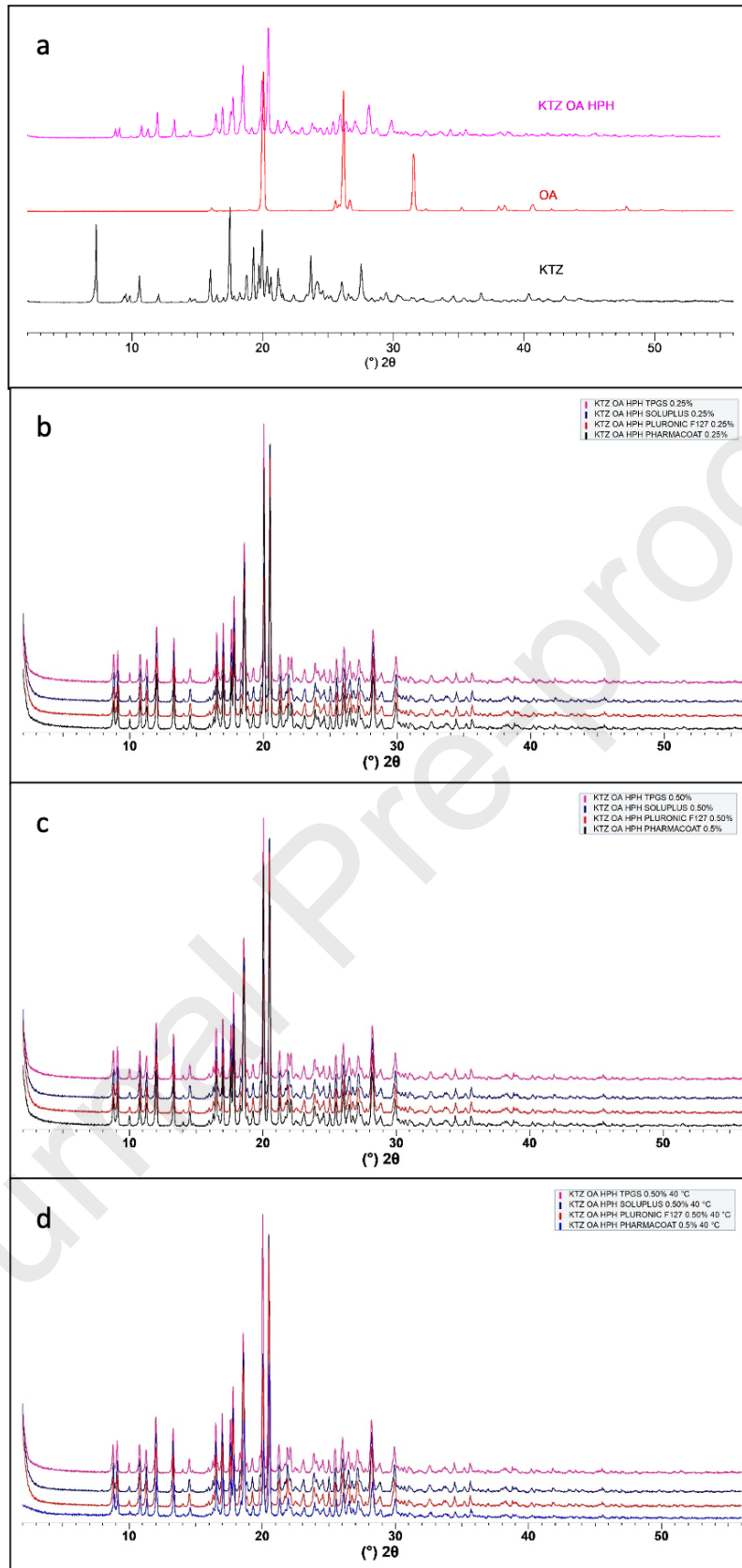
3 where KTZ presented a sharp endothermic melting point at 150 °C while for OA it was detected
4 at 192 °C respectively. The synthesized cocrystal of KTZ OA (1:1.1) produced through the
5 HPH process revealed a unique single endothermic peak at 197 °C.

6 From Fig. S1 it is obvious that no other endothermic event was noticed the melting peak of the
7 HPH processed materials was different to those of the parent materials, suggesting the
8 formation of a new crystalline structure. The comparison with the previously reported KTZ:OA
9 salt data from Martin *et al.* (2013), KTZ OA (1:1.1) showed a very similar melting point with
10 an endothermic peak at 198 °C which confirmed the formation of KTZ oxalate salt via HPH
11 [25]. Similarly, DSC analysis was carried out for the samples where stabilisers (Pharmacoat,
12 Pluronic, Soluplus and TPGS) were dissolved in the aqueous phase which was used for the HPH
13 process. Notably, the thermal behaviour of the newly formed crystals was similar to initially
14 HPH processed KTZ:OA, in the absence of any stabiliser. As shown in Fig. 1 all stabilisers
15 resulted in the formation of oxalate salt with sharp endothermic peaks at 197 °C. As shown in
16 Table 2 the stabilizers presented similar solubility parameter (δ) to bulk KTZ and hence the $\Delta\delta$
17 was <7 [32-35]. However, the DSC analysis showed that the stabilisers have no effect on the
18 KTZ solubilisation for concentrations varying from 0.25-0.50% and eventually in the purity of
19 the synthesised cocrystals. As previously mentioned HPH processing was also performed at
20 40°C to investigate the effect of stabilisers at elevated temperatures. Similarly, the utilization
21 of higher processing temperatures in combination with the applied pressure during the HPH
22 process did not affect the formation of the oxalate salts where sharp melting endotherms
23 appeared at the same temperature.

24 Furthermore, the bulk materials and products obtained by HPH were also analysed by PXRD
25 to identify variations in the diffraction patterns. The obtained data were compared with
26 previously reported results from the Cambridge Structural Database (CSD) using TOPAS
27 software. The degree of correspondence between the newly acquired crystal data and the CSD
28 reference data was evaluated through Rietveld refinement performed with TOPAS V4.2.
29 Although visual agreement of the crystalline peaks is important for assessing the quality of fit,
30 it is generally accepted that a refinement is satisfactory when the weighted profile R factor
31 (Rwp) is within approximately three times the expected R factor (Rexp) [36]. The principal
32 diffraction peaks for KTZ were observed at 2θ values of 7.28°, 9.50°, 10.69°, 11.96°, 16.13°,
33 17.50°, 20.01°, and 27.65° (Table 2). The salt former, OA, exhibited diffraction peaks at
34 16.09°, 19.03°, 20.11°, 26.24°, and 31.57° 2θ .

35 As presented in Fig. 2a, distinct and well-defined crystalline profiles were obtained for the
36 KTZ :OA salts following HPH processing. For the synthesized salt characteristic peaks
37 observed at 2θ values of 8.75°, 10.81°, 11.95°, 13.27°, 17.72°, 18.50°, 19.89°, 20.42°, and
38 28.14°. The diffraction peaks recorded for the formed oxalate differed significantly from those
39 of the bulk KTZ and OA crystals, confirming the formation of a new crystalline phase.
40 Furthermore, comparison of the obtained KTZ :OA diffractograms with the reference data
41 reported in the Cambridge Structural Database (CSD) by Martin *et al.* [25] revealed close
42 agreement in peak positioning. This correspondence was further verified through Rietveld
43 refinement, where the weighted profile R factor (Rwp) was found to be within twice the
44 expected R factor (Rexp) (Fig. S2, supplementary), indicating an excellent fit between the
45 experimental and simulated data. Similarly, X-ray powder diffraction (XRPD) analysis was
46 carried out on the HPH-processed samples prepared in the presence of stabilizers at
47 concentrations of 0.25% and 0.5% (Fig. 2b, c). The obtained diffractograms displayed identical

1 diffraction patterns, with consistent peak intensities and positions at the same 2θ values,
2 irrespective of the stabilizer concentration used. Moreover, as shown in Fig. 2d, the samples
3 processed with 0.5% stabilizer at elevated HPH temperatures (40 °C) exhibited diffraction
4 profiles comparable to those obtained under standard conditions. These findings indicate that
5 neither the concentration of stabilizers nor moderate increases in processing temperature
6 significantly influenced the crystalline structure or phase purity of the HPH-derived salts,
7 suggesting high process reproducibility and structural stability of the resulting solid forms.
8 Overall, the XRPD analysis confirmed the successful formation of KTZ :OA salts via HPH,
9 with the resulting crystalline solids exhibiting high phase purity and structural uniformity
10 approaching 100%.



1

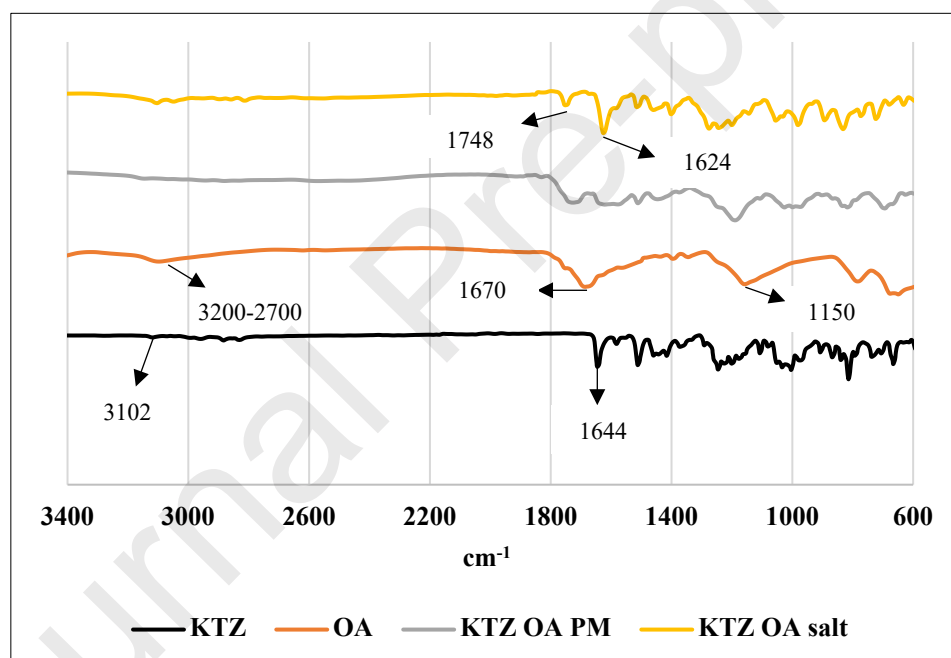
2 Fig.2: diffraction patterns of a) bulk KTZ, OA, and KTZ-OA salt, b) KTZ-OA salts processed
 3 with HPH in the presence of 0.25% stabilizers at 25°C, c) KTZ-OA salts processed with HPH
 4 in the presence of 0.50% stabilizers at 25°C, and d) KTZ-OA salts processed with HPH in the
 5 presence of 0.5% stabilizers at 40°C

1

2 3.3 FTIR spectroscopy analysis

3 Fourier-transform infrared (FT-IR) spectra of bulk ketoconazole (KTZ), oxalic acid (OA), their
 4 physical mixture (PM), and the KTZ:OA salt obtained via HPH processing were collected to
 5 investigate possible molecular interactions between KTZ and OA. Comparison of the spectra
 6 between bulk materials and the synthesized salt was performed to confirm proton transfer
 7 between the salt former and the drug. As shown in Fig. 3, KTZ exhibited a characteristic broad
 8 N–H stretching vibration at 3125 cm^{-1} , while absorption bands at 1644 and 1370 cm^{-1}
 9 corresponded to carbonyl (C=O) stretching and C=C stretching of the aromatic ring,
 10 respectively [37-42]

11 OA, containing two carboxylic acid ($-\text{COOH}$) groups, showed typical vibrational modes
 12 including O–H stretching, C=O stretching, C–O stretching, and both in-plane and out-of-plane
 13 O–H deformation vibrations. The O–H stretching band appeared in the $3200\text{--}2700\text{ cm}^{-1}$ region,
 14 with a prominent peak at 1670 cm^{-1} attributed to C=O stretching, and the C–O stretching
 15 vibration identified at 1150 cm^{-1} [43, 44].



16

17 **Fig. 3:** FTIR spectroscopic analysis of bulk materials and KTZ-OA salt produced by HPH.

18

19 In the FT-IR spectrum of the HPH synthesised KTZ:OA salt the C=O stretching band of KTZ
 20 shifted to 1624 cm^{-1} , accompanied by the emergence of a new peak at 1748 cm^{-1} . These shifts
 21 in vibrational frequencies for both KTZ and OA are indicative of supramolecular heterosyntho
 22 n formation within the multicomponent salt. Additionally, the disappearance of the broad O–H
 23 stretching band of OA suggests the formation of hydrogen bonds in the KTZ:OA salt [39-41].
 24 Similar results were obtained for the salts synthesized in the presence of stabilizers (data not
 25 shown).

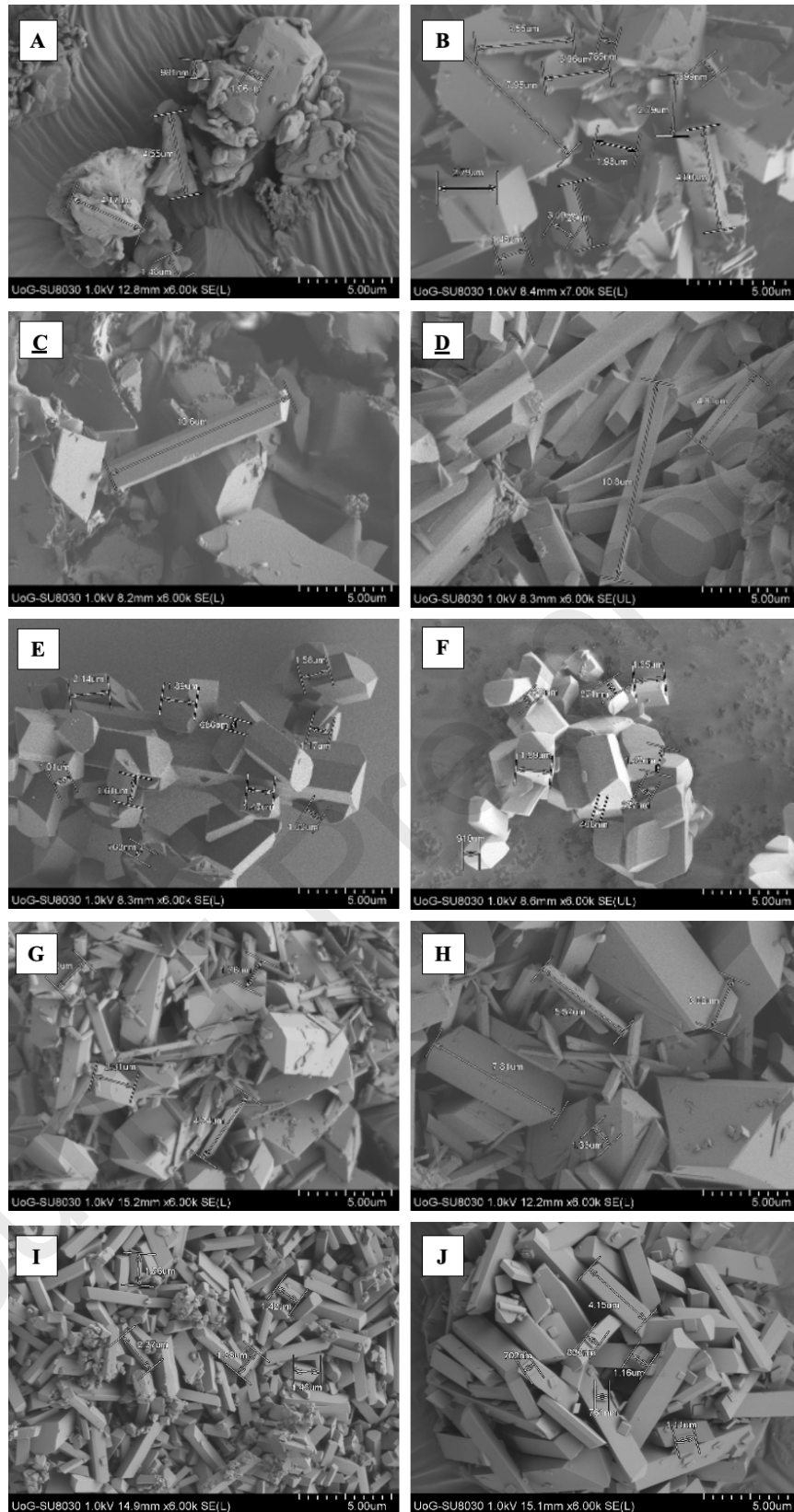
26

1 3.4 Morphology and particle size studies

2 Nanocrystals were characterized using a combination of imaging and non-imaging techniques,
3 with SEM selected for crystal size and morphology analysis due to precipitation issues
4 observed during light scattering measurements [45–47]. Bulk KTZ and HPH-synthesized KTZ-
5 OA salts were compared, revealing that the salts formed irregular block- or rod-shaped crystals,
6 with sizes ranging from 1 to 8 μm . A clear crystal lattice was observed in the KTZ-OA salts,
7 absent in bulk KTZ (Fig. 4b).

8 The effects of stabilizers on crystal morphology and size were evaluated using Pharmacoat®
9 606, Pluronic® F127, Soluplus®, and TPGS. Pharmacoat® 606 (Fig. 4, C, D) produced thin,
10 elongated rod-shaped crystals (nm to 4–10 μm), while Pluronic® F127 (Fig. 4, E, F) yielded
11 prismatic, elongated crystals with parallel flat faces, with particle sizes reduced to 0.3–2 μm .
12 Increasing Pluronic® F127 concentration [48] decreased crystal size further (Fig. 4, E, F).
13 Soluplus® resulted in irregular morphologies combining thin rods and larger blocks (2–8 μm),
14 showing minimal effect from concentration (Fig. 4, G, H)). TPGS stabilized slightly smaller
15 prismatic crystals with elongated shapes, ranging from nm to 1–4 μm (Fig. 4, I, J). Overall,
16 higher stabilizer concentrations produced smaller, more uniform crystals, consistent with prior
17 reports emphasizing the need for optimized stabilizer levels to prevent aggregation or Ostwald
18 ripening [49]. A 0.5% (w/v) stabilizer concentration was therefore selected for further studies.

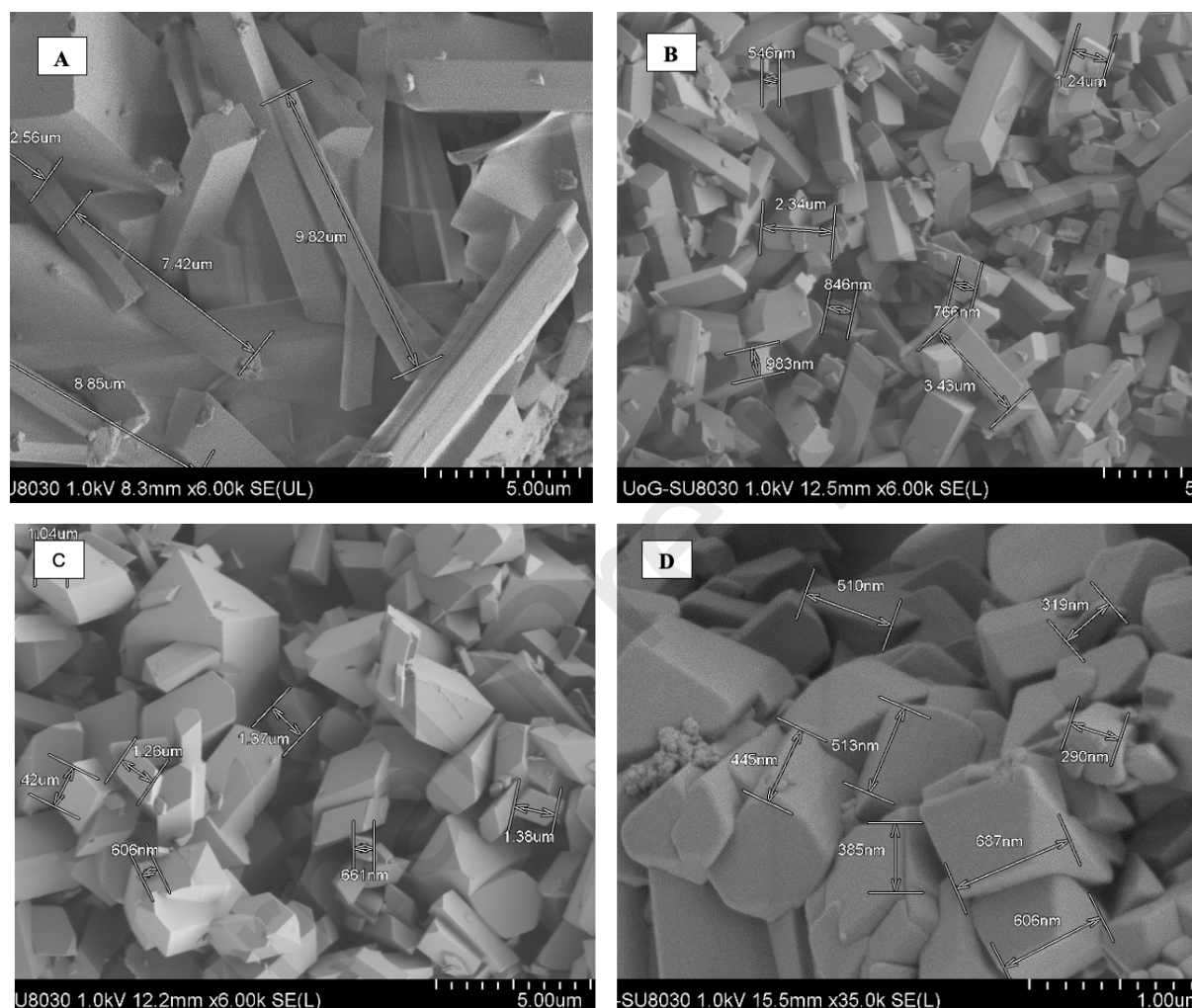
19 The impact of increasing HPH temperature from 25 °C to 40 °C was also examined.
20 Pharmacoat® 606 (Fig. 5A) produced longer rod-shaped crystals with minimal deformation,
21 while Soluplus® (Fig. 5B) and TPGS (Fig. 5C) yielded smaller, block-shaped crystals in the
22 nano- to micrometer range. Pluronic® F127 generated predominantly 0.3–0.6 μm short
23 prismatic crystals with minimal deformation (Fig. 5D).



1

2 **Fig. 4:** SEM images of bulk KTZ (A) and KTZ/OA HPH crystals without stabiliser (B), KTZ
 3 OA – Pharmacoat® 606; 0.25% (C) and 0.5% (D); KTZ OA- Pluronic® F127; 0.25% (E) and
 4 0.5% (F); KTZ OA- Soluplus®; 0.25% (G) and 0.5% (H); KTZ OA- TPGS; 0.25% (I) and
 5 0.50% (J).

1 During HPH, crystal agglomeration depends on activation energy, which stabilizers increase
 2 through steric and electrostatic mechanisms. Long-chain polymers create a physical barrier,
 3 whereas charged polymers reduce surface charge, both limiting aggregation [50, 51]. Particle
 4 size reduction was consistent across homogenization cycles and applied pressure [52]. Unlike
 5 previous reports of Pluronic® F127 destabilization at higher temperatures [53], the high-
 6 pressure environment likely inhibited micelle formation. The stabilizers were introduced at the
 7 beginning of the process, further supporting effective crystal size stabilization.



8
 9 **Fig. 5:** SEM images of KTZ OA salt produced by HPH process with Pharmacoat® (A),
 10 Soluplus® (B), TPGS (C) and Pluronic® F127 (D) at 40 °C.

11

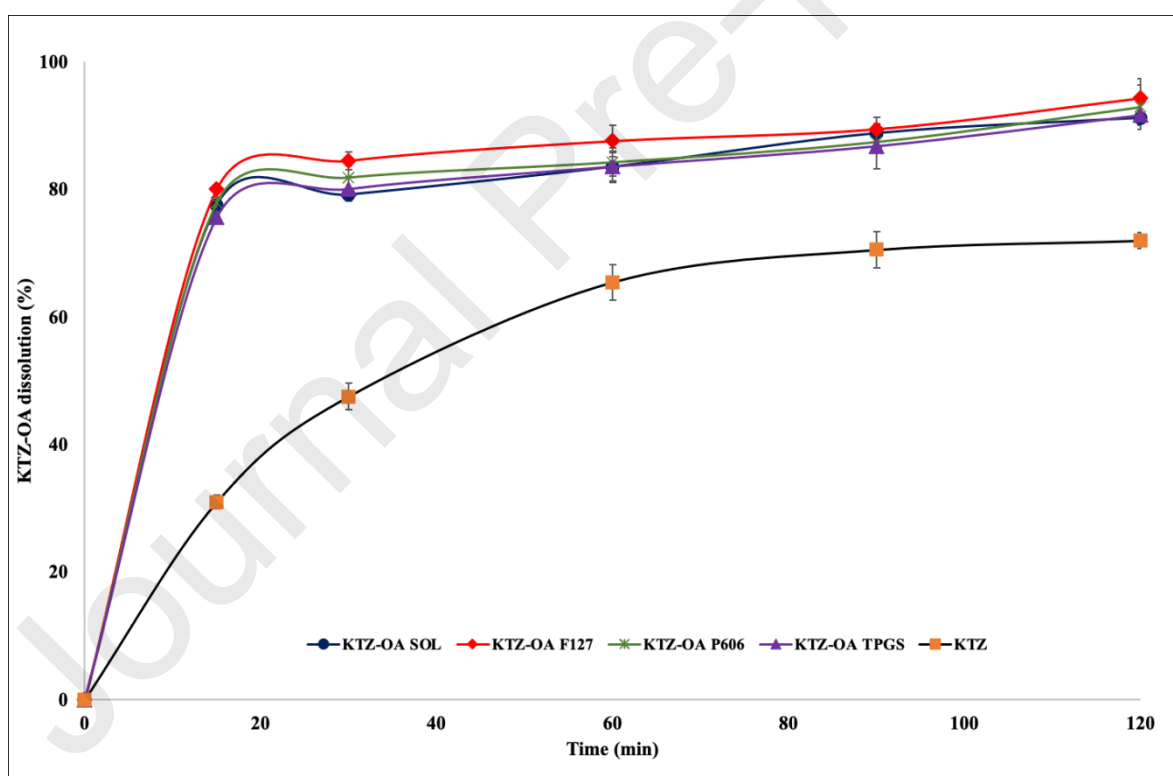
12 3.5. *In-vitro* dissolution studies

13 The dissolution behaviour of KTZ:OA salts homogenized with four different stabilizers at 40
 14 °C was evaluated against bulk KTZ over a 120 min period to assess the impact of nanosizing
 15 and salt formation on dissolution performance. **KTZ is known to exhibit pH-dependent
 16 solubility as weak base, dissolving readily in acidic environments (1-3) but demonstrating
 17 limited solubility under neutral and alkaline conditions [54, 55]. The dissolution rates in the
 18 pH range of 1–3, where no significant differences were observed between the parent compound
 19 and its salt forms. Therefore, dissolution studies were conducted at pH 4.4 to better differentiate**

1 the performance of the synthesized KTZ salts. Similar trends, with slightly lower dissolution
2 rates, were also observed at pH 6.8 (unpublished data).

3 As shown in Fig. 6, all KTZ:OA salts co-processed with 0.5% (w/v) stabilizers exhibited a
4 markedly faster dissolution rate compared with the parent compound. Bulk KTZ showed
5 sluggish dissolution, reaching only 47% after 30 min and not exceeding 72% after 120 min. In
6 contrast, the KTZ:OA salts displayed rapid dissolution within the first 15 min, achieving
7 between 72% and 80% release.

8 The enhanced dissolution performance of the KTZ:OA salts can be attributed to a combination
9 of factors, including reduced particle size, increased surface area, and improved wettability
10 resulting from stabilizer adsorption during the high-pressure homogenization process.
11 Moreover, the formation of the KTZ:OA salt likely modified the crystal lattice energy,
12 contributing to improved solubility relative to the bulk drug. Interestingly, the nature of the
13 stabilizer had minimal influence on the dissolution kinetics, suggesting that once a critical
14 stabilizer concentration was reached, further improvements were dominated by intrinsic
15 properties of the salt form rather than interfacial effects. Similar dissolution profiles were
16 obtained for the KTZ:OA salts prepared with 0.25% (w/v) stabilizers (data not shown),
17 indicating that both concentrations provided sufficient stabilization and surface modification
18 to achieve enhanced drug release.



19
20 **Fig. 6:** Release profile of bulk KTZ and KTZ:OA salts co-processed with Pharmacoat®,
21 Soluplus®, TPGS and Pluronic® F127 using HPH (the bars represent the STDV for the three
22 different dissolution runs that was carried out for each sample).

23 The KTZ–OA salt samples were stored under long-term stability conditions (25 °C/65% RH)
24 and analysed by XRPD after 6 and 12 months; the results are summarised in Table 3. Rietveld
25 refinement indicated that the crystalline purity remained unchanged at both time points and

1 was comparable to that of the as-prepared sample. The 12-month stability evaluation
 2 demonstrated no significant alteration in the crystal behaviour of the salts produced via HPH
 3 processing when stored at 25 °C/65% RH. Nevertheless, a comprehensive stability study
 4 conducted under appropriate ICH-recommended conditions is required to further confirm these
 5 findings.

6 **Table 3:** Comparison of KTZ:OA salt purity for as-made, and under 6 and 12-months storage
 7 stability.

Sample	Cocrystal purity (%)	
	6M 25°C/65% RH	12M 25°C/65% RH
KTZ: OA	99.9	99.9
KTZ: OA:Pharmacoat®	99.9	99.9
KTZ: OA:Soluplus®	99.9	99.9
KTZ: OA : Pluronic®	99.9	99.9
KTZ: OA:TPGS	99.9	99.9

8

9 4. Conclusions

10 The work demonstrates, for the first time, the feasibility of high-pressure homogenization as a
 11 direct synthesis route for pharmaceutical salts in the micro- to nanoscale range. This process
 12 integrates particle size reduction, salt formation, and stabilization in a single, solvent-free step,
 13 representing a significant advancement over traditional solid-state and solution-based
 14 crystallization methods. The ability to modulate crystal morphology and purity through simple
 15 control of processing parameters and stabilizer selection underscores the technique's
 16 formulation adaptability and scalability. The superior dissolution performance of the KTZ:OA
 17 salts further confirms the potential of HPH-derived materials to enhance the bioavailability of
 18 poorly soluble drugs. Collectively, these results position HPH as a next-generation platform
 19 for nanocrystal and salt engineering, enabling greener and more efficient pharmaceutical
 20 manufacturing.

21

22 Conflict of interests

23 The authors have no conflict of interest.

1
2
3
4
5
6
7
8
9
10
11
12
13
14
15
16
17
18
19
20
21
22
23
24
25
26
27
28
29
30
31
32
33
34
35
36
37
38
39
40
41
42
43
44
45
46

Acknowledgements

This project has received funding from the Interreg 2 Seas programme 2014-2020 co-funded by the European Regional Development Fund under subsidy contract 2S01-059_IMODE.

5. References

1. Shegokar R, Müller RH. Nanocrystals: Industrially feasible multifunctional formulation technology for poorly soluble actives. *Int J Pharm.* 2010;399(1-2):129-139.
2. Keck CM, Mu RH. Drug nanocrystals of poorly soluble drugs produced by high pressure homogenisation. *Eur J Pharm Biopharm.* 2006;62(1):3-16.
3. Shegokar R, Singh KK. Surface modified nevirapine nanosuspensions for viral reservoir targeting: In vitro and in vivo evaluation. *Int J Pharm.* 2011;421(2):341-352.
4. Malamataris M, Taylor KMG, Malamataris S, Douroumis D, Kachrimanis K. Pharmaceutical nanocrystals: production by wet milling and applications. *Drug Discov Today.* 2018;23(3):534-547.
5. Douroumis D, Fahr A. *Drug Delivery Strategies for Poorly Water-Soluble Drugs.* Wiley & Sons; 2013.
6. Mithu MDSH, Economidou S, Trivedi V, Bhatt S, Douroumis D. Advanced methodologies for pharmaceutical salt synthesis. *Cryst Growth Des.* 2021;21(2):1358-1374.
7. Malamataris M, Ross SA, Douroumis D, Velaga SP. Experimental cocrystal screening and solution-based scale-up cocrystallization methods. *Adv Drug Deliv Rev.* 2017.
8. Chadha R, Singh P, Khullar S, Mandal SK. Ciprofloxacin hippurate salt: crystallization tactics, structural aspects, and biopharmaceutical performance. *Cryst Growth Des.* 2016;16(9):4960-4967.
9. Serajuddin ATM. Salt formation to improve drug solubility. *Adv Drug Deliv Rev.* 2007;59(7):603-616.
10. Martin F, Pop M, Borodi G, Filip X, Kacso I. Ketoconazole salt and co-crystals with enhanced aqueous solubility. *Cryst Growth Des.* 2013;13(10):4295-4304.
11. Almeida e Sousa L, Reutzel-Edens SM, Stephenson GA, Taylor LS. Supersaturation potential of salt, co-crystal, and amorphous forms of a model weak base. *Cryst Growth Des.* 2016;16(2):737-748.
12. Elder DP, Holm R, De Diego HL. Use of pharmaceutical salts and cocrystals to address the issue of poor solubility. *Int J Pharm.* 2013;453(1):88-100.
13. M Akanda, MDSH Mithu, D Douroumis. Solid lipid nanoparticles: An effective lipid-based technology for cancer treatment. **Drug Deliv. Sci. and Techn.**, 104709
14. McClements DJ. Edible nanoemulsions: Fabrication, properties, and functional performance. *Soft Matter.* 2011;7(6):2297-2316.
15. Georget E, Miller B, Callanan M, Heinz V, Mathys A. (Ultra) High Pressure Homogenization for Continuous High Pressure Sterilization of Pumpable Foods- A Review. *Front Nutr.* 2014;1:1-6.
16. Diels AMJ, Michiels CW. High-pressure homogenization as a non-thermal technique for the inactivation of microorganisms. *Crit Rev Microbiol.* 2006;32(4):201-216.
17. Fernández-Ronco MP, Kluge J, Mazzotti M. High pressure homogenization as a novel approach for the preparation of co-crystals. *Cryst Growth Des.* 2013;13(5):2013-2024.

- 1 18. Loh ZH, Samanta AK, Sia Heng PW. Overview of milling techniques for improving
2 the solubility of poorly water-soluble drugs. *Asian J Pharm Sci.* 2014;10(4):255-274.
- 3 19. Lee J, Choi JY, Park CH. Characteristics of polymers enabling nano-comminution of
4 water-insoluble drugs. *Int J Pharm.* 2008;355(1-2):328-336.
- 5 20. Tuomela A, Hirvonen J, Peltonen L. Stabilizing agents for drug nanocrystals: Effect on
6 bioavailability. *Pharmaceutics.* 2016;8(16):1-18.
- 7 21. Liu P, Viitala T, Kartal-Hodzic A, et al. Interaction studies between indomethacin
8 nanocrystals and PEO/PPO copolymer stabilizers. *Pharm Res.* 2015;32(2):628-639.
- 9 22. Lu Y, Wang ZH, Li T, McNally H, Park K, Sturek M. Development and evaluation of
10 transferrin-stabilized paclitaxel nanocrystal formulation. *J Control Release.*
11 2014;176(1):76-85.
- 12 23. Mittapelly N, Rachumallu R, Pandey G, et al. Investigation of salt formation between
13 memantine and pamoic acid: Its exploitation in nanocrystalline form as long acting
14 injection. *Eur J Pharm Biopharm.* 2016;101:62-71.
- 15 24. Homayouni A, Sadeghi F, Varshosaz J, Afrasiabi Garekani H, Nokhodchi A. Promising
16 dissolution enhancement effect of soluplus on crystallized celecoxib obtained through
17 antisolvent precipitation and high pressure homogenization techniques. *Colloids*
18 *Surfaces B Biointerfaces.* 2014;122:591-600.
- 19 25. Martin FA, Pop MM, Borodi G, Filip X, Kacso I. Ketoconazole salt and co-crystals
20 with enhanced aqueous solubility. *Cryst Growth Des.* 2013;13(10):4295-4304.
- 21 26. Hiendrawan S, Hartanti AW, Veriansyah B, Widjojokusumo E, Tjandrawinata RR.
22 Solubility Enhancement of Ketoconazole Via Salt and Cocrystal Formation. *Int J*
23 *Pharm Pharm Sci.* 2015;7(7):160-164.
- 24 27. Production of Itraconazole Nanocrystal-Based Polymeric Film Formulations for
25 Immediate Drug Release.” *Pharmaceutics.* 2020;12(10):960
- 26 28. Ige PP, Baria RK, Gattani SG. “Fabrication of fenofibrate nanocrystals by probe
27 sonication method for enhancement of dissolution rate and oral bioavailability.”
28 *Colloids Surf B: Biointerfaces.* 2013;108:366-373
- 29 29. Vadher B, Shah S, Dudhat K, Dhaval M, Sing S, Prajapati BG. “Ketoconazole
30 Nanocrystals Fortified Gel for Improved Transdermal Applications.” *Nanofabrication.*
31 2024;9:1885
- 32 30. SG Potta, S Minemi, RK Nukala, C Peinado, DA Lamprou, A Urquhart . Preparation
33 and characterization of ibuprofen solid lipid nanoparticles with enhanced solubility.
34 *Journal of microencapsulation* 28 (1), 74-81
- 35 31. WS Schlindwein, M Gibson. *Pharmaceutical quality by design: a practical approach*
36 John Wiley & Sons.
- 37 32. Jinjiang Li, Doris Chiappetta. An investigation of the thermodynamic miscibility
38 between VeTPGS and polymers. *Int. J. Pharm.*, 2008, 350 (1–2), 212-219
- 39 33. Jiannan Lu, Kristina Cuellar, Nathan I. Hammer, Seongbong Jo, Andreas Gryczke, Karl
40 Kolter, Nigel Langley, and Michael A. Repka. Solid-state Characterization of
41 Felodipine-Soluplus® Amorphous Solid Dispersions. *Drug. Del. Ind. Pharm.* 2016,
42 (42)3, 485-496
- 43 34. Sandra Jankovica, Georgia Tsakiridou, Felix Ditzingera, Niklas J. Koehle, Daniel J.
44 Pricel, Alexandra-Roxana Iliee, Lida Kalantzi, Kristof Kimpe, Ren, Holm, Anita Nair,
45 Brendan Griffine, Christoph Saal, Martin Kuentz. Application of the solubility
46 parameter concept to assist with oral delivery of poorly water-soluble drugs – a
47 PEARL review. *Journal of Pharmacy and Pharmacology*, 71 (2019), pp. 441–463
- 48 35. Teja Kitak, Aleksandra Dumicic , Odon Planinšek, Rok Šibanc, Stanko Srcic.
49 Determination of Solubility Parameters of Ibuprofen and Ibuprofen Lysinate.
50 *Molecules* 2015, 20, 21549–21568

- 1 36. Toby BH. R factors in Rietveld analysis: how good is good enough? *Powder Diffr.*
2 2006;21(1):67–70.
- 3 37. Tiago JM, Padrela L, Rodrigues MA, Matos HA, Almeida AJ, de Azevedo EG. Single-
4 step co-crystallization and lipid dispersion by supercritical enhanced atomization. *Cryst*
5 *Growth Des.* 2013;13:4940–4947.
- 6 38. Bezerra RDS, Domingos FNB, dos Santos AO, da Silva LM, Ayala AP, Souto EB, da
7 Silva LFL, de Sousa FF, Lang R, de Oliveira Neto JG. A novel ethionamide–phthalic
8 acid salt with improved dissolution for tuberculosis therapy: insights from structural,
9 spectroscopic, and DFT-periodic calculations analyses. *Cryst Growth Des.*
10 2025;25(15):6345–6361.
- 11 39. Elder EJ, Evans JC, Scherzer BD, Hitt JE, Kupperblatt GB, Saghir SA, Markham DA.
12 Preparation, characterization, and scale-up of ketoconazole with enhanced dissolution
13 and bioavailability. *Drug Dev Ind Pharm.* 2007;33(7):755–765.
- 14 40. Patel MR, Patel RB, Parikh JR, Solanki AB, Patel BG. Investigating effect of
15 microemulsion components: in vitro permeation of ketoconazole. *Pharm Dev Technol.*
16 2011;16(3):250–258.
- 17 41. Kamble RN, Bothiraja C, Mehta PP, Varghese V. Synthesis, solid state characterization
18 and antifungal activity of ketoconazole cocrystals. *J Pharm Investig.* 2017;48(5):541-
19 549.
- 20 42. Shayanfar A, Jouyban A. Physicochemical characterization of a new cocrystal of
21 ketoconazole. *Powder Technol.* 2014;262:242-248.
- 22 43. Muthuselvi C, Arunkumar A, Rajaperumal G. Growth and Characterization of Oxalic
23 Acid Doped with Tryptophan Crystal for Antimicrobial Activity. *Der Chem Sin.*
24 2016;7(4):55-62.
- 25 44. Alatas F, Ratih H, Soewandhi SN. Enhancement of solubility and dissolution rate of
26 telmisartan by telmisartan-oxalic acid co-crystal formation. *Int J Pharm Pharm Sci.*
27 2015;7(3):423-426.
- 28 45. Peltonen L, Tuomela A, Hirvonen J. Polymeric Stabilizers for Drug Nanocrystals.
29 *Handb Polym Pharm Technol.* 2015;4:67-87.
- 30 46. Cerdeira AM, Mazzotti M, Gander B. Formulation and drying of miconazole and
31 itraconazole nanosuspensions. *Int J Pharm.* 2013;443:209-220.
- 32 47. Peltonen L. Practical guidelines for the characterization and quality control of pure drug
33 nanoparticles and nano-cocrystals in the pharmaceutical industry. *Adv Drug Deliv Rev.*
34 2018;131:101-115.
- 35 48. Schwarz C, Mehnert W. Solid lipid nanoparticles (SLN) for controlled drug delivery
36 II. drug in corporation and physicochemical characterization. *J Microencapsul.*
37 1999;16(2):205-213.
- 38 49. Ito A, Konnerth C, Schmidt J, Peukert W. Effect of polymer species and concentration
39 on the production of mefenamic acid nanoparticles by media milling. *Eur J Pharm*
40 *Biopharm.* 2016;98:98-107.
- 41 50. Van Eerdenbrugh B, Van den Mooter G, Augustijns P. Top-down production of drug
42 nanocrystals: Nanosuspension stabilization, miniaturization and transformation into
43 solid products. *Int J Pharm.* 2008;364(1):64-75.
- 44 51. Verwey EJ. Theory of the stability of lyophobic colloids. *J. Phys. Chem.* 1947;
45 51(3):631-636.
- 46 52. Müller R, Junghanns. Nanocrystal technology, drug delivery and clinical applications.
47 *Int J Nanomed.* 2008;3(3):295-309.
- 48 53. Deng J, Huang L, Liu F. Understanding the structure and stability of paclitaxel
49 nanocrystals. *Int J Pharm.* 2010;390(2):242-249.

- 1 54. Adachi M, Hinatsu Y, Kusamori K, et al. Improved dissolution and absorption of
2 ketoconazole in the presence of organic acids as pH-modifiers. *Eur J Pharm Sci.*
3 2015;76:225-230.
4 55. Chen YM, Rodríguez-Hornedo N. Cocrystals Mitigate Negative Effects of High pH on
5 Solubility and Dissolution of a Basic Drug. *Cryst Growth Des.* 2018;18(3):1358-1366.
6

7
8
9
10 **Declaration of interests**
11

12 The authors declare that they have no known competing financial interests or personal
13 relationships that could have appeared to influence the work reported in this paper.

14
15 The authors declare the following financial interests/personal relationships which may be
16 considered as potential competing interests:
17

18
19
20
21
22



